

[*Supporting Information*]

Synthesis of pyridine-based covalent organic framework as efficient adsorbent for rhodamine B removal

Kejian Chang,* Huijuan Huang, Yuandong Meng, Zidan Ju, Haiyan Song, Liang
Zhang, Xiaoqin Niu, Zhi-Jun Li*

*College of Petrochemical Engineering, Longdong University, Qingyang, Gansu,
745000, P. R. China.*

E-mail: *kejianchang_chem@163.com, lizhj_chem@163.com*

Table of Contents

Section I. Materials and Instrumentation

Section II. Synthetic procedures and characterizations of TAPP- DBTA-COF and TAPP-DBTA-COP.

Section III. Adsorption experiments

Section IV. References

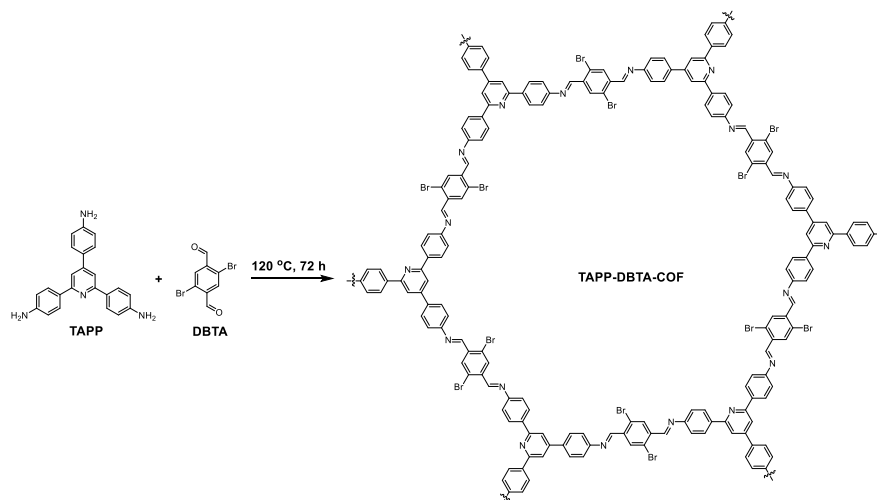
Section I. Materials and Instrumentation

All chemicals and solvents were commercially sourced and used without further purification. Deionized water was used throughout all experiments. 2,4,6-tris(4-aminophenyl)pyridine (TAPP) and 2,5-dibromobenzene-1,4-dicarbaldehyde (DBTA) were synthesized according to reported literature method.^{1,2}

Fourier transform Infrared (FT-IR) spectra were recorded on a Shimadzu 8400S instrument. Solid-state NMR measurements were carried out on a Bruker WB Avance III 400 MHz spectrometer. Powder X-ray diffraction (PXRD) patterns were collected on an Ultima IV X-ray diffractometer with Cu K α radiation ($\lambda = 0.15406$ nm) and operated at 40 kV and 40 mA. Scanning Electron Micrograph (SEM) images were obtained with a Zeiss Gemini 300 microscope operated at an accelerating voltage of 3.0 kV. Elemental analysis data was recorded on a Carlo-Erba EA-1110 instrument. The thermogravimetric analysis (TGA) were measured with a TGA5500 instrument over the temperature range of 30 to 800 °C with a heating rate of 10 °C/min under nitrogen atmosphere. The nitrogen adsorption and desorption isotherms were measured at 77 K using a Micromeritics ASAP 2460 system. The surface area was calculated from the adsorption data using Brunauer-Emmett-Teller (BET) method. UV-vis spectra were recorded on an Agilent Cary 60 Spectrophotometer. X-ray photoelectron spectroscopy (XPS) data were recorded with an ESCALAB 250Xi spectrometer (ThermoFisher Scientific).

Section II. Synthetic procedures and characterizations of TAPP-DBTA-COF and TAPP-DBTA-COP.

Synthesis of TAPP-DBTA-COF.



2,4,6-tris(4-aminophenyl)pyridine (188 mg, 0.5 mmol), 2,5-dibromobenzene-1,4-dicarbaldehyde (233 mg, 0.8 mmol) and 6 mL *o*-dichlorobenzene/mesitylene (4 mL/2 mL) were charged into a 20 mL vial. The resulting mixture was sonicated for 5 min and then 0.8 mL of 6 M acetic acid was added. The vial was sealed and heated at 120 °C for 72 h. The precipitate was collected by filtration and washed with dichloromethane, acetone, methanol respectively. Further purification was conducted *via* Soxhlet extraction with THF for 12 h. After being dried at 80°C for 10 h, the final **TAPP-DBTA-COF** was obtained as a yellow powder in 85% yield. **Elemental Analysis:** calcd. for C₇₀H₄₀N₈Br₆: C, 57.10; H, 2.74; N, 7.61. Found: C, 56.04; H, 2.64; N, 7.89.

Synthesis of TAPP-DBTA-COP.

2,4,6-tris(4-aminophenyl)pyridine (106 mg, 0.30 mmol), 2,5-dibromobenzene-1,4-dicarbaldehyde (131 mg, 0.45 mmol) and 8 mL DMSO were charged into a 50 mL vial. The resulting mixture was heated at 80 °C for 24 h. After that, the precipitate was collected by filtration and washed with dichloromethane, acetone, methanol respectively. Further purification was conducted *via* Soxhlet extraction with THF for 12 h. After being dried at 80°C for 10 h, the final **TAPP-DBTA-COP** was obtained as

a pale brown powder in 83% yield. **Elemental Analysis:** calcd. for $C_{70}H_{40}N_8Br_6$: C, 57.10; H, 2.74; N, 7.61. Found: C, 55.72; H, 2.82; N, 7.92.

The deviations in elemental analysis of TAPP-DBTA-COF and TAPP-DBTA-COP may be caused by trace amounts solvent trapped in porous network.

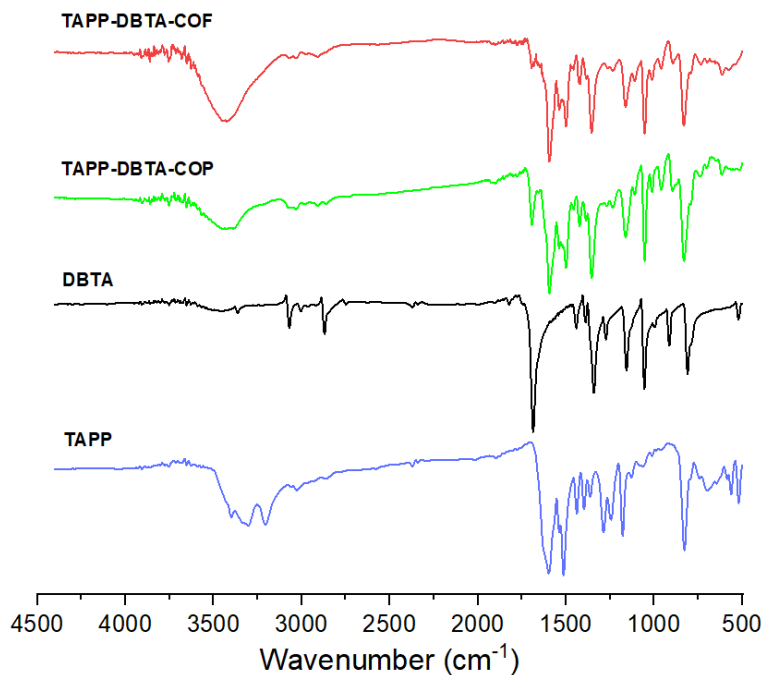


Fig. S1. FT-IR spectra of TAPP-DBTA-COF, TAPP-DBTA-COP and monomers.

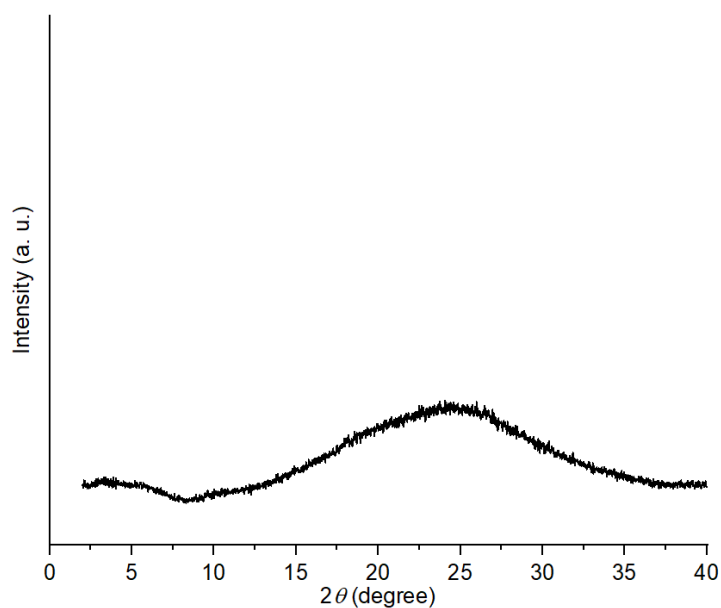


Fig. S2. PXRD patterns of TAPP-DBTA-COP.

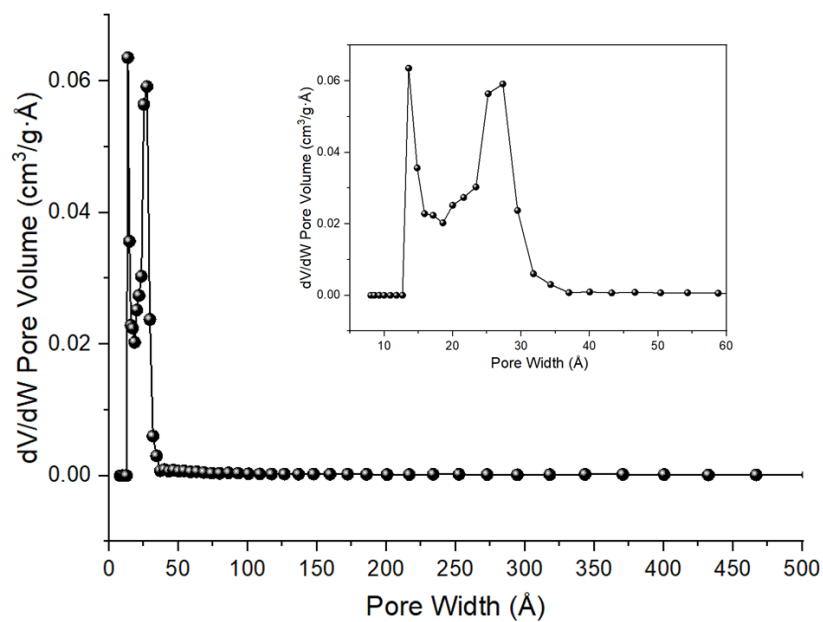


Fig. S3. Pore diameter of TAPP-DBTA-COF calculated from desorption isotherm with DFT method.

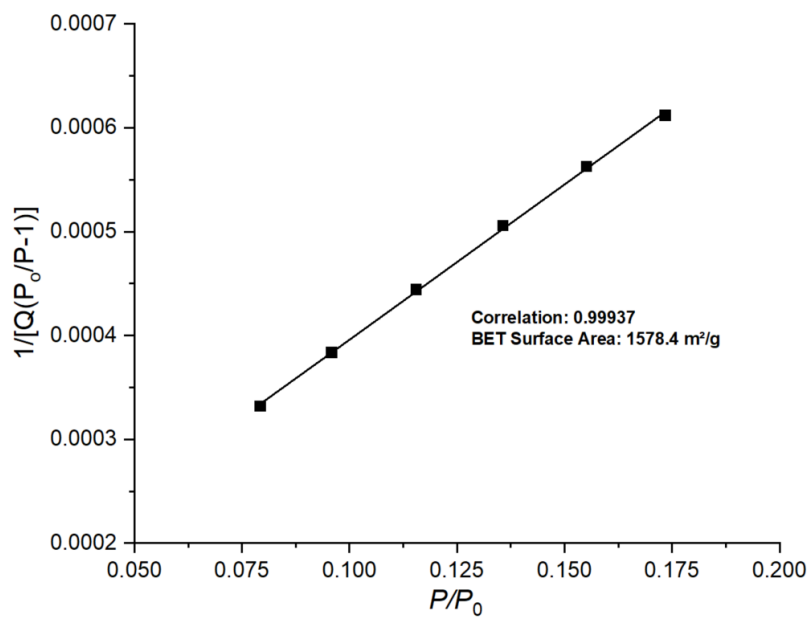


Fig. S4. BET surface area plot of TAPP-DBTA-COF.

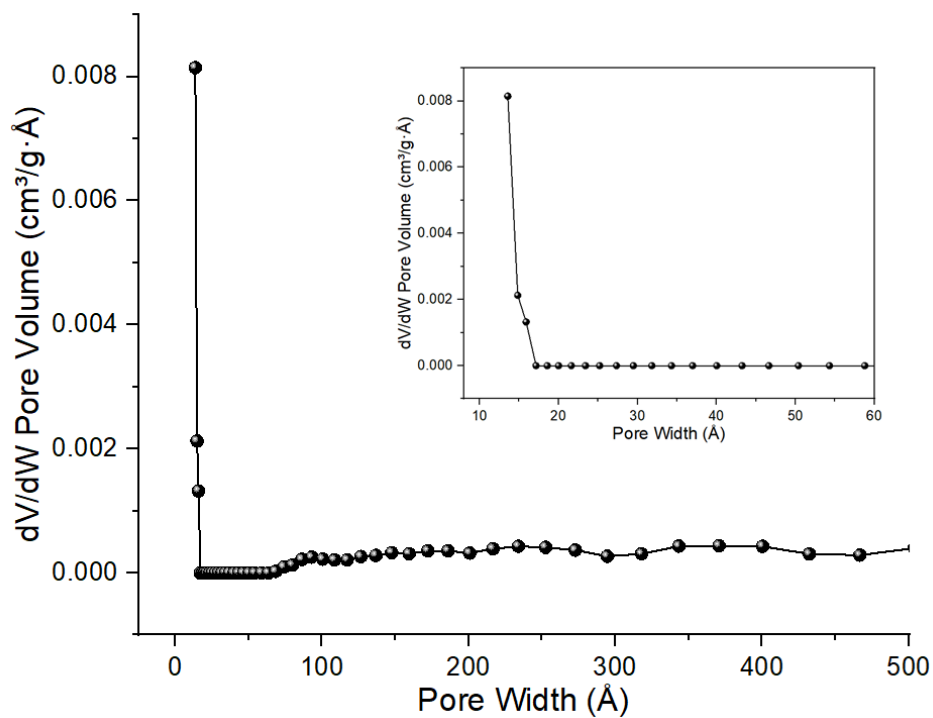


Fig. S5. Pore diameter of TAPP-DBTA-COP calculated from desorption isotherm with DFT method.

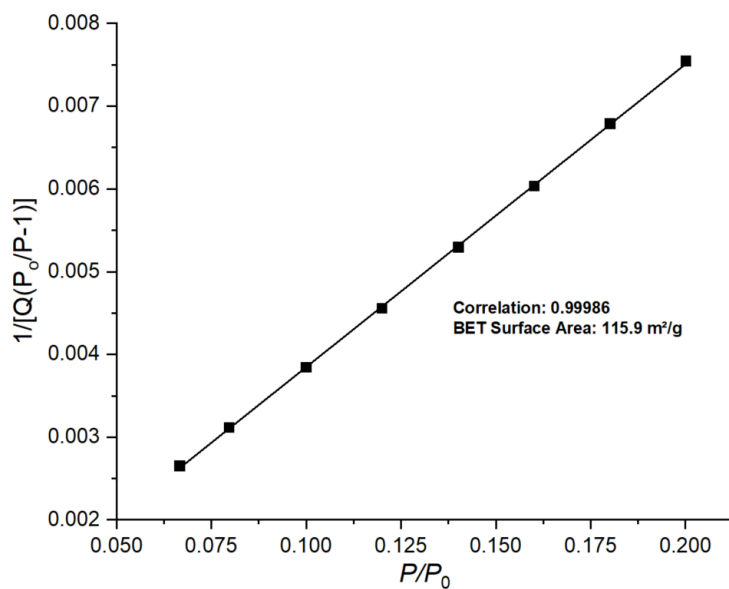


Fig. S6. BET surface area plot of TAPP-DBTA-COP.

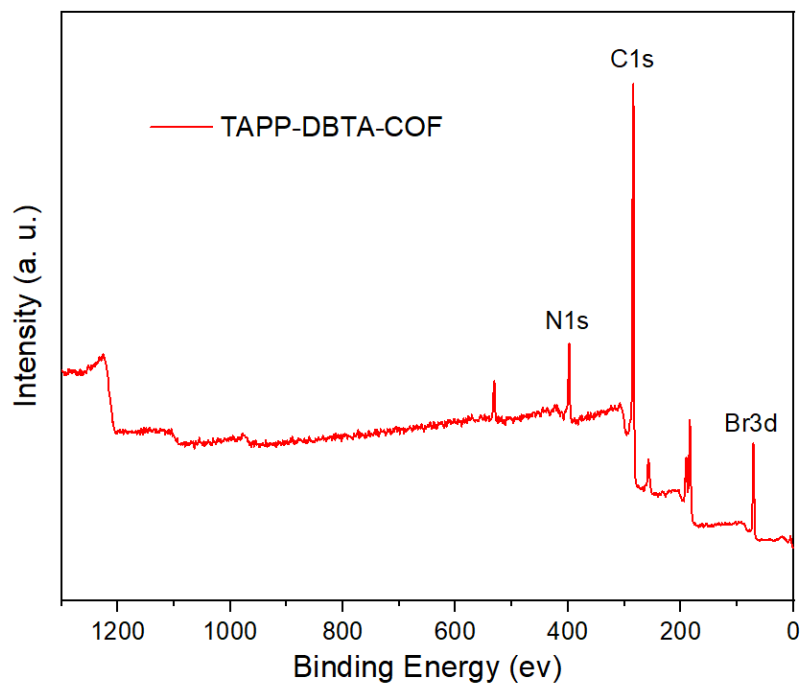


Fig. S7. XPS survey spectra of TAPP-DBTA-COF.

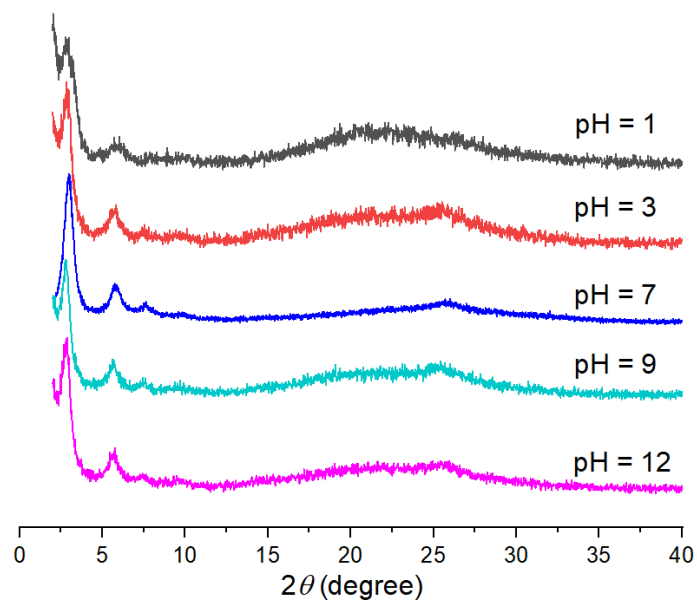


Fig. S8. PXRD patterns of TAPP-DBTA-COF before and after treatment with different aqueous solutions (pH = 1, 3, 7, 9, 12).

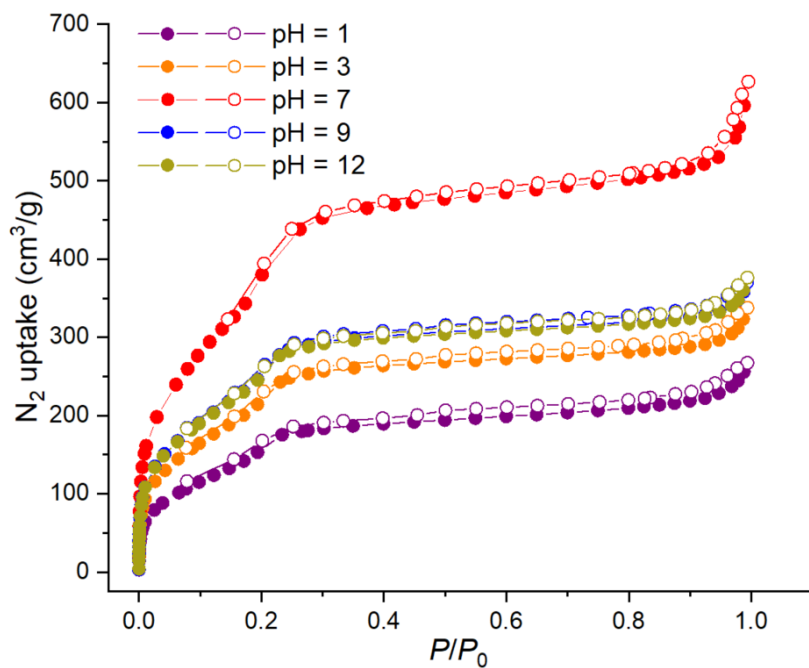


Fig. S9. Nitrogen sorption isotherm curves of TAPP-DBTA-COF before and after treatment with different aqueous solutions (pH = 1, 3, 7, 9, 12). The BET surface areas were 664.7, 933.5, 1578.4, 1036.3 and 1053.0 $m^2 g^{-1}$, respectively.

Table S1. Fractional atomic coordinates for the unit cell of TAPP-DBTA-COF.

Space group: <i>P2/m</i> $a = 38.7109 \text{ \AA}$, $b = 3.5765 \text{ \AA}$, $c = 35.7454 \text{ \AA}$, $\alpha = \gamma = 90^\circ$, $\beta = 117.4762^\circ$							
Atom	X (Å)	Y (Å)	Z (Å)	Atom	X (Å)	Y (Å)	Z (Å)
C1	-0.1587	0	1.20326	H32	-0.04349	0	1.12984
N2	-0.14142	0	1.17768	H33	-0.08246	0	1.16675
C3	-0.1331	0	1.25019	C34	-0.03372	0	1.05747
C4	-0.09225	0	1.26603	H35	-0.01447	0	1.091
C5	-0.06732	0	1.30946	C36	-0.01634	0	1.02821
C6	-0.08217	0	1.3384	C37	0.02443	0	1.04369
C7	-0.12283	0	1.32319	C38	0.0404	0	1.01571
C8	-0.14795	0	1.27972	Br39	0.05998	0	1.10271
H9	-0.0794	0	1.24474	H40	0.07185	0	1.02869
H10	-0.03604	0	1.32097	C41	-0.22255	0	1.14008
N11	-0.05479	0	1.38258	C42	-0.19967	0	1.18448
H12	-0.13567	0	1.34435	C43	-0.26692	0	1.11951
H13	-0.17876	0	1.27022	C44	-0.28735	0	1.14387
C14	-0.0626	0	1.41435	C45	-0.3281	0	1.12478
H15	-0.09232	0	1.40943	C46	-0.35017	0	1.08105
C16	-0.03069	0	1.45821	C47	-0.33077	0	1.05616
C17	-0.03884	0	1.49283	C48	-0.29	0	1.07499
C18	-0.00844	0	0.534	H49	-0.27295	0	1.1778
Br19	-0.09086	0	1.48608	H50	-0.34291	0	1.14416
H20	-0.01575	0	0.55987	N51	-0.39193	0	1.06375
C21	-0.16133	0	1.13487	H52	-0.34659	0	1.02214
C22	-0.20231	0	1.11565	H53	-0.27767	0	1.05347
C23	-0.13847	0	1.11039	C54	-0.41753	0	1.02406
C24	-0.15616	0	1.06579	H55	-0.40858	0	0.99954
C25	-0.1334	0	1.04462	C56	-0.45974	0	1.0116
C26	-0.09277	0	1.06686	C57	-0.48769	0	0.9687
C27	-0.07478	0	1.11122	C58	0.47261	0	0.95744
C28	-0.09737	0	1.13256	Br59	-0.47363	0	0.92389
H29	-0.18733	0	1.04649	H60	0.45191	0	0.92417
H30	-0.14737	0	1.01044	H61	0.21325	0	0.79548
N31	-0.0714	0	1.04288	H62	0.21793	0	0.91793

Section III. Organic dyes adsorption experiments

Sorption kinetics study

Typically, TAPP-DBTA-COF or TAPP-DBTA-COP (3 mg) was dispersed in 5 mL Rh B aqueous solution (200 ppm) and stirred under room temperature. After stirring for a desired time, the sorbent was filtered with a syringe filter (PTFE, 0.45 μm), and the solution was detected by UV-vis spectrophotometer. The adsorption percentage was obtained by comparing the maximum absorbance ($\lambda = 554 \text{ nm}$) with the original Rh B aqueous solution.

$$Q_t = \left(\frac{C_0 - C_t}{m} \right) \times V$$

where Q_t is the adsorption capacity at contact time t , C_0 is the initial concentration of Rh B solution, C_t is the concentration of Rh B at time t , m is the mass of TAPP-DBTA-COF or TAPP-DBTA-COP, and the V is the volume of Rh B aqueous solution.

Two kinetic models, including pseudo-first order model and pseudo-second order model were used to fit the sorption kinetics data. These two models can be expressed in the following equations:

Pseudo-first order equation:

$$Q_t = Q_e - Q_e e^{-k_1 t}$$

Pseudo-second order equation:

$$Q_t = \frac{K_2 Q_e^2 t}{1 + k_2 Q_e t}$$

where k_1 and k_2 ($\text{g mg}^{-1} \text{ min}^{-1}$) are the rate constants of pseudo-first order and pseudo-second order, respectively.

Sorption isotherm study

The sorption isotherm experiments of TAPP-DBTA-COF and TAPP-DBTA-COP were conducted by varying the initial concentrations of Rh B (400-2200 ppm for TAPP-DBTA-COF, or 40-120 ppm for TAPP-DBTA-COP). Typically, adsorbent (5 mg) was

dispersed in 6 mL Rh B aqueous solution. The solution was stirred for 2.5 h under room temperature, and then the solution was filtered with a syringe filter (PTFE, 0.45 μm). After being diluted with deionized water, the solution was measured with UV-vis spectrophotometer. The equilibrium adsorption capacity (Q_e) was calculated by using the following equation.

$$Q_e = \left(\frac{C_0 - C_e}{m} \right) \times V$$

where the C_e is the equilibrium concentration of Rh B solution.

The adsorption isotherm curves of Rh B were fitted by LangmuirEXT1, Langmuir, and Freundlich models respectively.

LangmuirEXT1 equation:

$$Q_e = \frac{Q_m K_S C_e^\gamma}{1 + K_S C_e^\gamma}$$

Langmuir equation:

$$Q_e = \frac{Q_m K_L C_e}{1 + K_L C_e}$$

Freundlich equation:

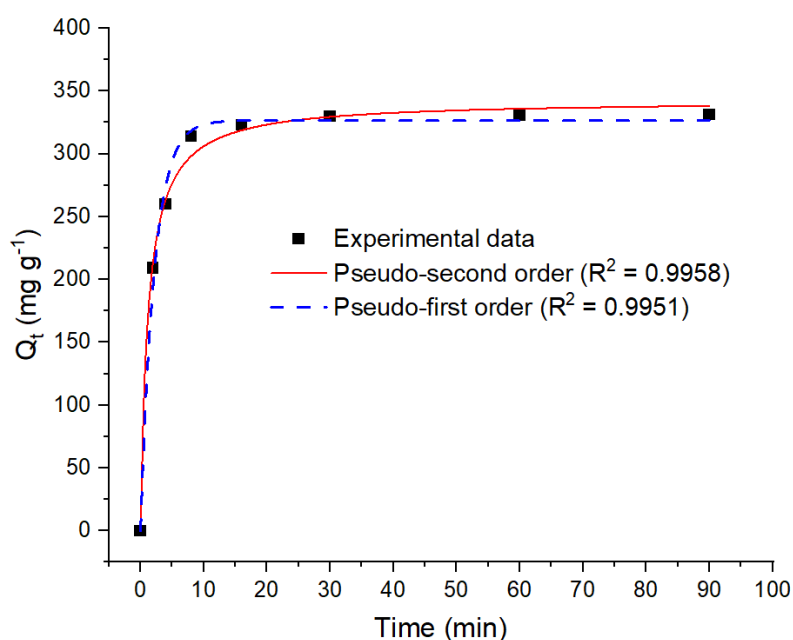
$$Q_e = K_F C_e^{1/n}$$

where Q_m is the maximum adsorption capacity, K_S and γ are the constants of LangmuirEXT1 model, K_L is the constant of Langmuir model, K_F and n are constants of Freundlich model.

The influence of pH value of the solution was studied by dispersing TAPP-DBTA-COF (5 mg) in 6 mL Rh B aqueous solution (1400 ppm) with different pH values (pH = 1, 3, 7, 9, 12). The pH values of the solution were adjusted *via* adding 0.1 M HCl or 0.1 M NaOH. After stirring for 2 hours, the sorbent was filtered with a syringe filter (PTFE, 0.45 μm), and the solutions were detected by UV-vis spectrophotometer, the adsorption percentage was determined based on the intensity reduction of the

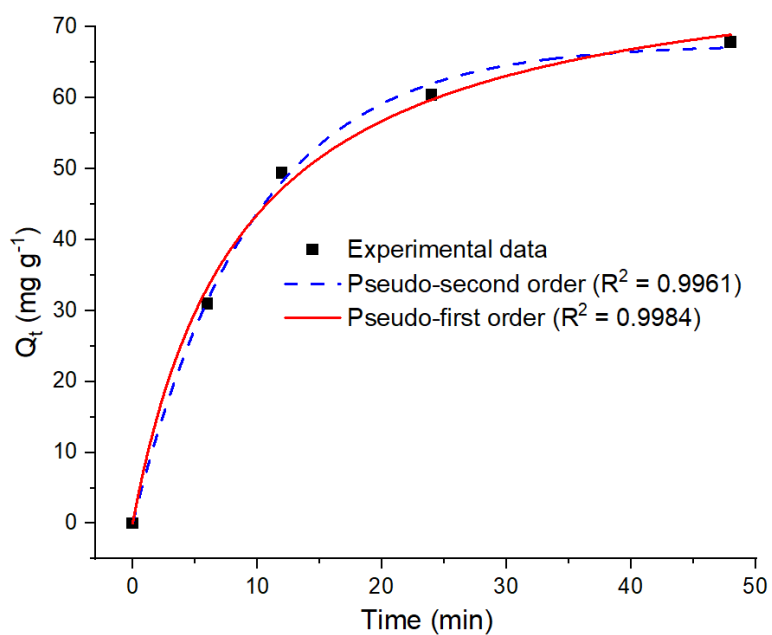
characteristic peak of Rh B.

The recyclability of TAPP-DBTA-COF was studied in an amplified experiment. 28 mg of TAPP-DBTA-COF was dispersed in 40 mL Rh B aqueous solution (1400 ppm), and stirred for adsorption. The adsorbed Rh B can be desorbed *via* directly eluting with ethanol until the eluent was changed to colorless. The ethanol solution was collected and detected by UV-vis spectrophotometer to determine desorption efficiency. After thoroughly washing with ethanol, the regenerated adsorbent TAPP-DBTA-COF-Regenerated was obtained and dried at 80 °C. The next adsorption cycle was performed under the same conditions.



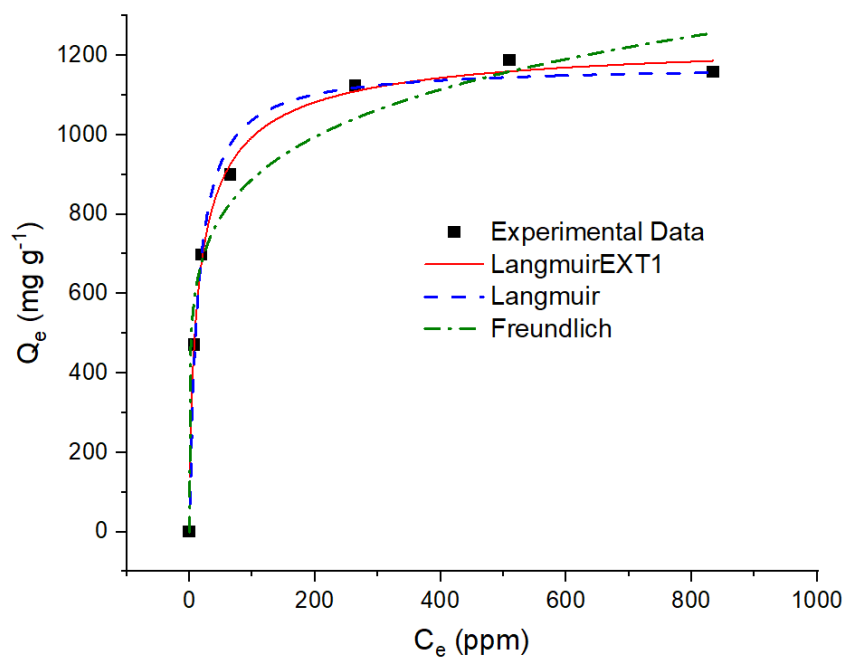
Fitting model	Parameter	correlation coefficient
Pseudo-first order	$Q_e = 326.6 \text{ mg g}^{-1}$ $k_1 = 0.460 \text{ min}^{-1}$	$R^2 = 0.9951$
Pseudo-second order	$Q_e = 342.7 \text{ mg g}^{-1}$ $k_2 = 0.00244 \text{ g mg}^{-1} \text{ min}^{-1}$	$R^2 = 0.9958$

Fig. S10. The kinetics for adsorption of Rh B by TAPP-DBTA-COF fitted by pseudo-first and pseudo-second order models respectively.



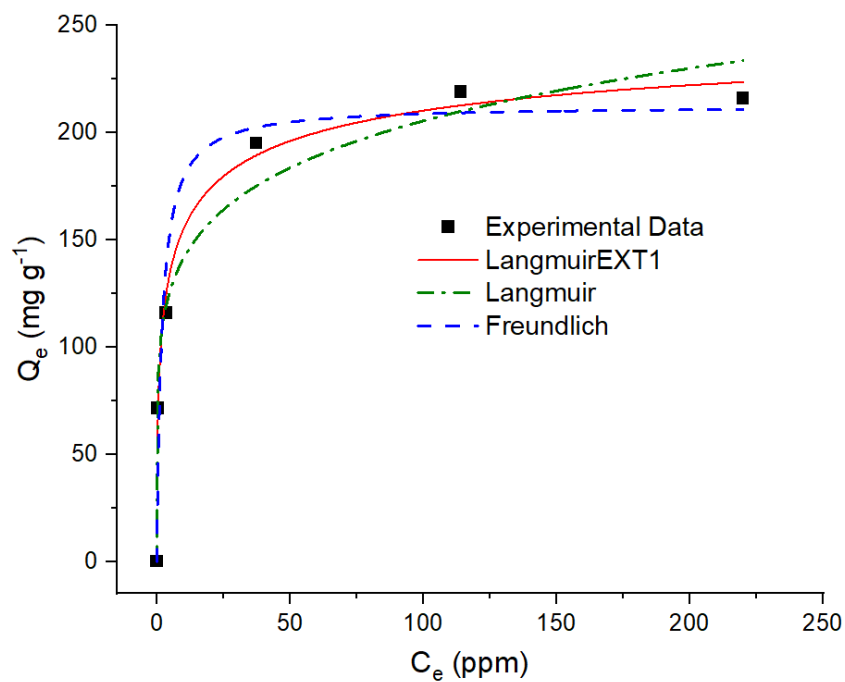
Fitting model	Parameter	correlation coefficient
Pseudo-first order	$Q_e = 67.5 \text{ mg g}^{-1}$ $k_1 = 0.104 \text{ min}^{-1}$	$R^2 = 0.9984$
Pseudo-second order	$Q_e = 81.4 \text{ mg g}^{-1}$ $k_2 = 0.00141 \text{ g mg}^{-1} \text{ min}^{-1}$	$R^2 = 0.9961$

Fig. S11. The kinetics for adsorption of Rh B by TAPP-DBTA-COP fitted by pseudo-first and pseudo-second order models respectively.



Fitting model	Parameter	correlation coefficient
LangmuirEXT1	$Q_m = 1254.1 \text{ mg g}^{-1}$ $K_s = 0.14$ $\gamma = 0.72$	$R^2 = 0.9924$
Langmuir	$Q_m = 1174.6 \text{ mg g}^{-1}$ $K_L = 0.08$	$R^2 = 0.9919$
Freundlich	$K_F = 418.6$ $n = 6.12$	$R^2 = 0.9689$

Fig. S12. The adsorption isotherm of Rh B by TAPP-DBTA-COF fitted with three different models. As listed above, LangmuirEXT1 model displayed a better correlation coefficient than other two models, suggesting LangmuirEXT1 model can well describe the adsorption process.



Fitting model	Parameter	correlation coefficient
LangmuirEXT1	$Q_m = 263.7 \text{ mg g}^{-1}$ $K_s = 0.52$ $\gamma = 0.44$	$R^2 = 0.9871$
Langmuir	$Q_m = 212.7 \text{ mg g}^{-1}$ $K_L = 0.53$	$R^2 = 0.9514$
Freundlich	$K_F = 97.22$ $n = 6.15$	$R^2 = 0.9765$

Fig. S13. The adsorption isotherm of Rh B by TAPP-DBTA-COP fitted with three different models. As listed above, LangmuirEXT1 model displayed a better correlation coefficient than other two models, suggesting LangmuirEXT1 model can well describe the adsorption process.

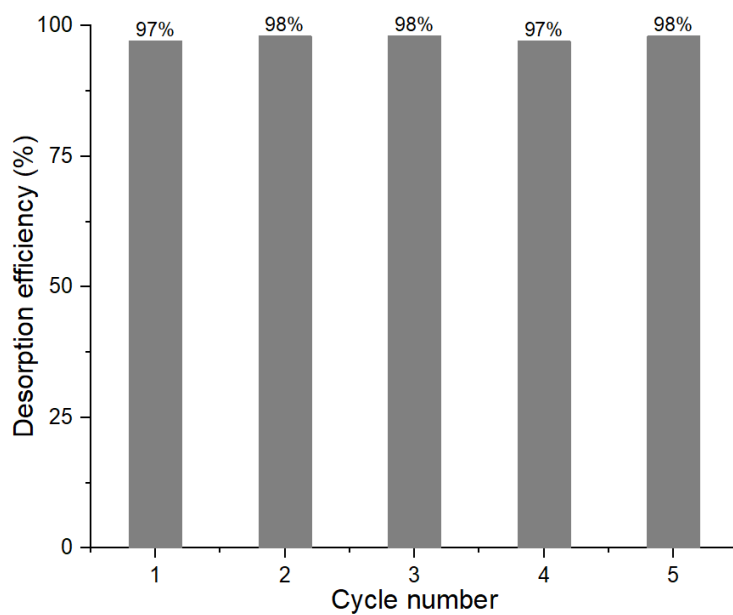


Fig. S14. Desorption efficiency of Rh B on TAPP-DBTA-COF with ethanol after each cycle.

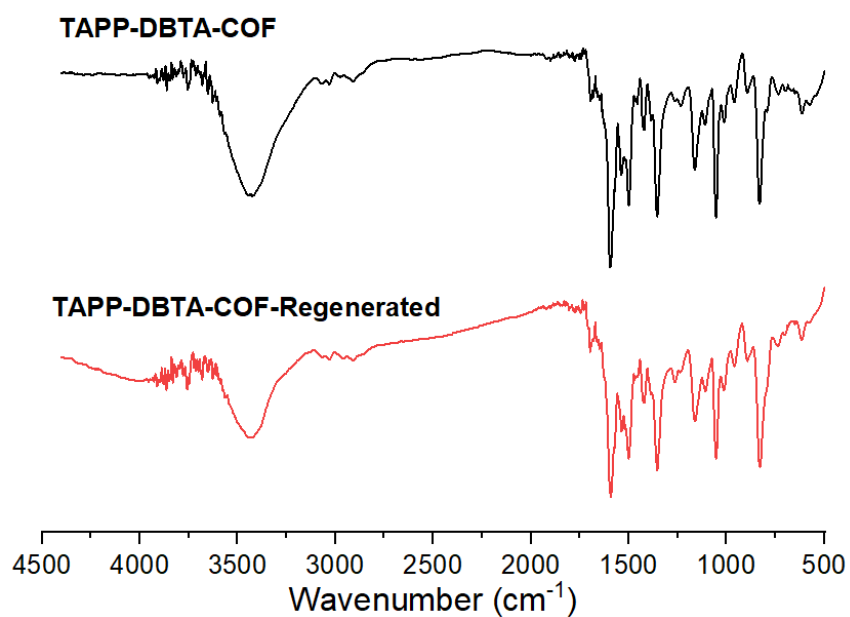


Fig. S15. FT-IR spectra of TAPP-DBTA-COF and TAPP-DBTA-COF-Regenerated.

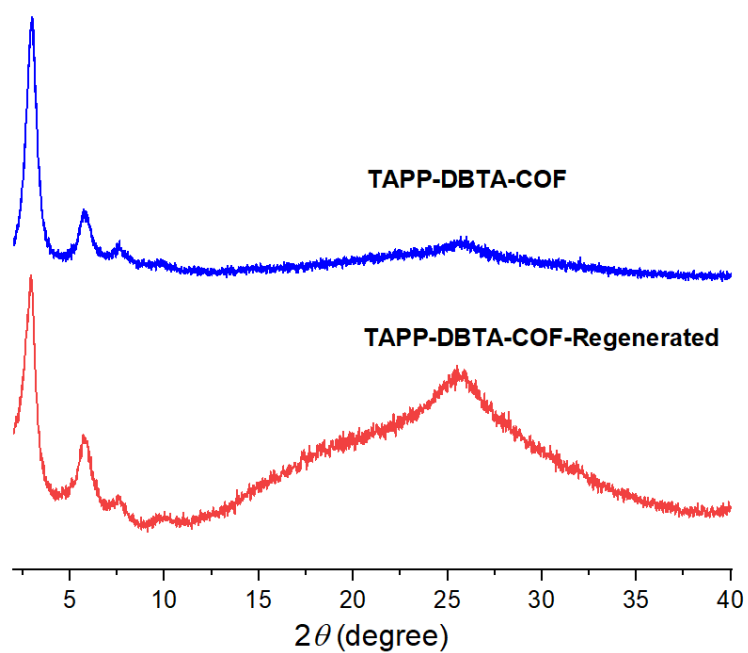


Fig. S16. PXRD patterns of TAPP-DBTA-COF and TAPP-DBTA-COF-Regenerated.

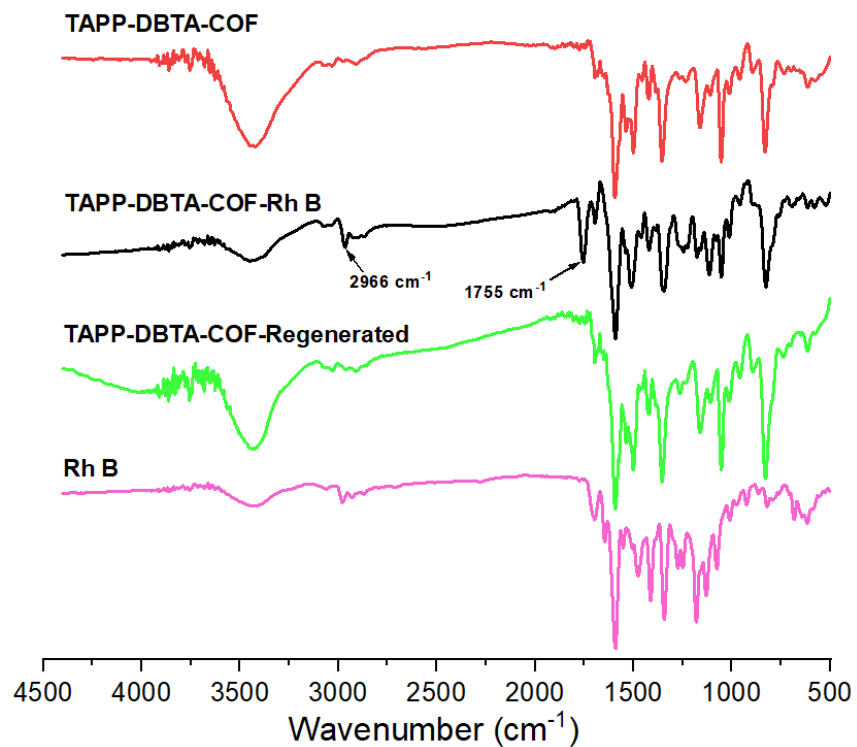


Fig. S17. FT-IR spectra of TAPP-DBTA-COF, TAPP-DBTA-COF-Rh B, TAPP-DBTA-COF-Regenerated and Rh B.

Section IV. References

- (1) Shen, D.; Liu, J.; Yang, H.; Yang, S. Highly Thermally Resistant and Flexible Polyimide Aerogels Containing Rigid-rod Biphenyl, Benzimidazole, and Triphenylpyridine Moieties: Synthesis and Characterization. *Chem. Lett.* **2013**, *42*, 1545-1547.
- (2) Deng, Y.; Zhang, Z.; Du, P. Y.; Ning, X. M.; Wang, Y.; Zhang, D. X.; Liu, J.; Zhang, S. T.; Lu, X. Q. Embedding Ultrasmall Au Clusters into the Pores of a Covalent Organic Framework for Enhanced Photostability and Photocatalytic Performance. *Angew. Chem., Int. Ed.* **2020**, *59*, 6082-6089.